	シンポジウム		
2014年	東海大学医学部付属病院 第4回医療連携セミナー	【講演】軟骨再生医療の現状と未来	佐藤正人
研究分担者　阿久津英憲			
2014年	12th Annual Meeting of ISSCR	Generation of committed neural progenitors from human fibroblasts by defined factors (F-2142)	Miura T, Sugawara T, Fukuda A, Tamoto R, Umezawa A, Akutsu H
2014年	第59回日本生殖医学会学術講演会	生殖医学における ES 細胞と iPS 細胞の意義	阿久津英憲
研究分担者　長嶋比呂志			
2014年	第41回日本臓器保存生物医学会学術集会	受精卵凍結保存のノウハウは組織・臓器の保存にどこまで応用可能か？	長嶋比呂志
研究分担者　加藤玲子			
2015年	The 54th Annual Meeting of the Society of Toxicology	Effects of metal oxide nanomaterials on cytotoxicity and immune response in THP-1 cells	Miyajima-Tabata A, Kawakami T, Komoriya K, Kato R, Niimi S, Isama K
2014年	Eurotox 2014	Cellular response of THP-1 cells cultured on the polymer biomaterials	Miyajima-Tabata A, Kato R, Komoriya K, Niimi S
2014年	第36回日本バイオマテリアル学会	ヒト単球系細胞の蛋白質発現挙動に基づく医用材料の血液適合性評価マーカの探索	加藤玲子, 酘島由二, 福井千恵, 比留間瞳, 澤田留美, 宮島敦子, 新見伸吾
2014年	第36回日本バイオマテリアル学会	血液適合性評価における HEMA/MEA ランダム共重合体材料に対する蛋白質マーカーの挙動について	宮島敦子, 小森谷薫, 田中賢, 加藤玲子, 新見伸吾
2014年	第41回日本毒性学会	酸化金属ナノマテリアルに対する THP-1 細胞の細胞応答	宮島敦子, 河上強志, 小森谷薫, 加藤玲子, 新見伸吾, 伊佐間和郎

Ⅴ．研究成果の刊行物・別刷

Ukai et al. BMC Musculoskeletal Disorders (2015) 16:35
DOI 10.1186/s12891-015-0499-0

BMC Musculoskeletal Disorders

RESEARCH ARTICLE Open Access

Diffusion tensor imaging can detect the early stages of cartilage damage: a comparison study

Taku Ukai[1], Masato Sato[1*], Tomohiro Yamashita[2], Yutaka Imai[2], Genya Mitani[1], Tomonori Takagaki[1], Kenji Serigano[1] and Joji Mochida[1]

Abstract

Background: In the present study, we measured damaged areas of cartilage with diffusion tensor (DT) imaging and T2 mapping, and investigated the extent to which cartilage damage could be determined using these techniques.

Methods: Forty-one patients underwent arthroscopic knee surgery for osteoarthritis of the knee, a meniscus injury, or an anterior cruciate ligament injury. Preoperative magnetic resonance imaging of the knee was performed, including T2 mapping and diffusion tensor imaging. The presence of cartilage injury involving the medial and lateral femoral condyles and tibia plateau was assessed during surgery using the Outerbridge scale. The ADC, T2 values and fractional anisotropy of areas of cartilage injury were then retrospectively analysed.

Results: The ADC results identified significant differences between Outerbridge grades 0 and 2 ($P = 0.041$); 0 and 3 ($P < 0.001$); 1 and 2 ($P = 0.045$); 1 and 3 ($P < 0.001$); and 2 and 3 ($P = 0.028$). The FA results identified significant differences between grades 0 and 1 ($P < 0.001$); 0 and 2 ($P < 0.001$); and 0 and 3 ($P < 0.001$). T2 mapping identified significant differences between Outerbridge grades 0 and 2 ($P = 0.032$); 0 and 3 ($P < 0.001$); 1 and 3 ($P < 0.001$); and 2 and 3 ($P < 0.001$). Both the T2 mapping ($R^2 = 0.7883$) and the ADC ($R^2 = 0.9184$) correlated significantly with the Outerbridge grade. The FA ($R^2 = 0.6616$) correlated slightly with the Outerbridge grade.

Conclusions: T2 mapping can be useful for detecting moderate or severe cartilage damage, and the ADC can be used to detect early stage cartilage damage. The FA can also distinguish normal from damaged cartilage.

Keywords: Magnetic resonance imaging, Diffusion tensor imaging, Apparent diffusion coefficient, Fractional anisotropy, T2 mapping, Cartilage, Osteoarthritis, Knee joint

Background

Osteoarthritis (OA) is caused by a range of factors, including age, genetic factors, mechanical stress, and cytokines. OA causes pain, range of motion limitations, and functional joint impairment. A particular characteristic of OA is a reduction in the amount of hyaline cartilage. Proteoglycan depletion and increased cartilage water content are observed initially in OA, and these changes are followed by decreased type II collagen and collagen fiber degradation [1]. As X-ray imaging is not an objective evaluation index based on articular cartilage, it is difficult to evaluate early cartilage damage and repair [2]. Early diagnosis and treatment are important because cartilage contains few cellular components and has a low self-restoration capacity.

In recent years, magnetic resonance imaging (MRI) has become useful for evaluating cartilage damage. Because it depicts cartilage tissue more clearly than X-ray imaging, MRI is used to facilitate multiplanar evaluation. Although standard MRI is relatively insensitive for detection of early cartilage injury, recent advances have improved its ability to evaluate biomechanical and biochemical elements in articular cartilage, including glycosaminoglycan, collagen, and water content. Various types of MRI systems are used for the noninvasive evaluation of cartilage damage, including delayed gadolinium-enhanced MRI of cartilage, T1ρ relaxation time, and ^{23}Na spectroscopic imaging. These systems measure proteoglycan depletion, and T2 mapping has the potential for evaluating cartilage water content and collagen

* Correspondence: sato-m@is.icc.u-tokai.ac.jp
[1]Department of Orthopaedic Surgery, Surgical Science, Tokai University School of Medicine, 143 Shimokasuya, Isehara, Kanagawa 259-1193, Japan
Full list of author information is available at the end of the article

fiber direction [3]. Increases in T2 with increased cartilage matrix damage, decreased collagen content, and increased water content have also been reported [3].

Diffusion tensor (DT) imaging is used to detect the water molecule diffusion process [4,5] and is now used to evaluate spinal cord injury [6] and cerebral infarction [7]. DT imaging has also recently been used in evaluation of cartilage damage [4,5]. The apparent diffusion coefficient (ADC) obtained by DT imaging reflects decreased proteoglycan and water content [5], whereas the fractional anisotropy (FA) reflects changes in collagen fiber alignment [5,8,9].

Few reports have investigated whether the Outerbridge grade of the cartilage damage can be assessed using MRI techniques. We graded cartilage damage assessed by arthroscopy according to the Outerbridge classification [10] (Table 1) and measured each grade of cartilage damage using DT imaging and T2 mapping. We also investigated the extent to which cartilage damage could be determined using the Outerbridge grade.

Methods

Population

Forty-one patients (14 men, 27 women; 13–78 years old, mean age 51.5 years) who underwent arthroscopic surgery at Tokai University Hospital from April 2010 through May 2011 were included in this study (Table 2). Patients who had undergone arthroscopic surgery were included, whereas patients who underwent total knee arthroplasty and open reduction and internal fixation without arthroscopy were excluded. We also excluded patients who had undergone arthroscopic surgery but had a small area of cartilage damage or mixed grades of cartilage damage, or in whom evaluation with MRI was difficult. The Tokai University Hospital Institutional Review Board for Clinical Research approved the study, and all patients signed the consent form.

Image and data analysis

MRI of the knee joint (T2 mapping and DT imaging) was performed on the day prior to the surgery. The sites of the cartilage injury were identified during arthroscopic surgery, and the relationships between the operative findings and the preoperative MRI values in these sites were investigated. When arthroscopic surgery was performed, the knee joint was divided into the following regions: inner femoral condyle, outer femoral condyle, inner tibial condyle, and outer tibial condyle. Three Japanese orthopedic specialists conducted the arthroscopic assessment of the cartilage injuries according to the Outerbridge classification [10] (Table 1).

The ROIs were measured at all levels, from the cartilage surface to the deep zones, and the subchondral bone was excluded carefully. Each ROI was measured within a range that measured 55 voxels high and 40 voxels wide [5,8] (Figure 1). We evaluated and recorded the Outerbridge grade of the damaged areas of cartilage during surgery, confirmed arthroscopic photographs during measurement of cartilage damage using MRI, and had another doctor reevaluate the Outerbridge grade. Three orthopaedic surgeons and one radiologist, having board

Table 1 Outerbridge classification

Grade	Property
0	Normal
1	Cartilage with softening and swelling
2	A partial-thickness defect with fissures on the surface that do not reach subchondral bone or exceed 1.5 cm in diameter
3	Fissuring to the level of subchondral bone in an area with a diameter more than 1.5 cm
4	Exposed subchondral bone

Table 2 Indication for operations and arthroscopic findings

Indication	No. of patients	Outerbridge grade	No. of patients
Osteoarthritis	17	0	29
ACL injury	11	1	31
Meniscus injury	7	2	21
Loose body	1	3	20
Osteochondritis dissecans	1		
Osteochondroma	1		
Osteonecrosis	1		
Pigmented villonodular synovitis	1		
Tibia platau fracture	1		

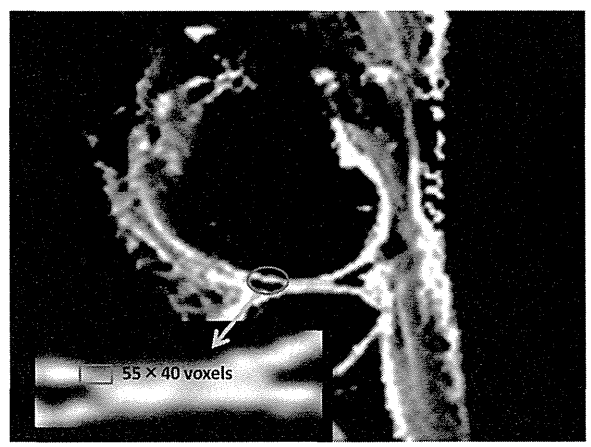

Figure 1 Region of interest (ROI) settings. The ROI was set in areas of arthroscopically confirmed cartilage damage, and the ADC, FA, and T2 were measured. The ROI was 55 voxels high and 40 voxels wide, and care was taken to measure all cartilage levels without including the subchondral bone.

certificate of The Japanese Orthopaedic Association and Japan Radiological Society, separately measured the areas of cartilage damage on the MRI. To minimize disparities, the measurements were obtained three times and the mean value calculated.

T2 mapping

T2 mapping was performed on an Achieva 3.0-T TX scanner (Philips Healthcare, Best, The Netherlands), with the patient's knees positioned within a TX SENSE Knee eight-channel coil (Philips Healthcare). Imaging was conducted under the following conditions: sequence, multiecho turbo spin-echo (TSE); field of view (FOV), 120 × 120 mm; matrix, 211 × 320; repetition time (TR), 2510 ms; echo time (TE), 16, 32, 48, 64, 80, 96, and 112 ms; turbo factor, 7; slice thickness, 5 mm; gaps, 1 mm; number of excitations (NEX), 1; water fat shift (WFS), 0.882 pixels/429.7 Hz; fat-suppression spectral presaturation with inversion recovery; and scan time, 8 min and 54 s.

DT imaging

Imaging was conducted under the following conditions: sequence, single-shot, spin-echo echo planar imaging (EPI); FOV, 150 × 150 mm; matrix, 144 × 144; TR, 2200 ms; TE, 68 ms; EPI factor, 73; number of slices, 13; slice thickness, 5 mm; gaps, 1 mm; NEX, 20; WFS, 28.628 pixels/15.2 Hz; fat-suppression spectral attenuated inversion recovery ; MPG, 6; b-value, 600; half-scan factor, 0.678; and scan time, 10 min and 34 s.

Data processing

From the DT imaging, the six components of the symmetric diffusion tensor were calculated [5]. For each voxel, the three eigenvalues ($\lambda1$, $\lambda2$, $\lambda3$) and their corresponding eigenvectors were calculated. The ADC and FA were calculated from the eigenvalues as follows [8,11,12]:

$$ADC = \frac{1}{3}(\lambda1 + \lambda2 + \lambda3),$$

$$FA = \sqrt{\frac{3}{2}\frac{(\lambda1-ADC)^2 + (\lambda2-ADC)^2 + (\lambda3-ADC)^2}{\lambda_1^2 + \lambda_2^2 + \lambda_3^2}}$$

Statistical analysis

One-way ANOVA followed by Tukey–Kramer post hoc tests was used to compare the ADC, FA, and T2 between Outerbridge grade. Spearman's rank correlation was used to identify significant relationships between the Outerbridge grade and the ADC, FA, and T2. P values of < 0.05 were considered significant.

Results

MRI findings

The ADC for each Outerbridge grade was grade 0, $1.37 \pm 0.14 \times 10^{-3}$ mm^2/s; grade 1, $1.41 \pm 0.26 \times 10^{-3}$ mm^2/s; grade 2, $1.63 \pm 0.25 \times 10^{-3}$ mm^2/s; and grade 3, $1.90 \pm 0.40 \times 10^{-3}$ mm^2/s. The FA for each Outerbridge grade was grade 0, 0.28; grade 1, 0.17; grade 2, 0.14; and grade 3, 0.16. The T2 for each Outerbridge grade was grade 0, 40.1 ± 3.4 ms; grade 1, 41.9 ± 5.5 ms; grade 2, 45.6 ± 7.6 ms; and grade 3, 63.8 ± 5.9 ms.

The ADC differed significantly between Outerbridge grades 0 and 2 ($P = 0.041$); 0 and 3 ($P < 0.001$); 1 and 2 ($P = 0.045$); 1 and 3 ($P < 0.001$); and 2 and 3 ($P = 0.028$; Figure 2a). The FA differed significantly between Outerbridge grades 0 and 1 ($P < 0.001$); 0 and 2 ($P < 0.001$); and 0 and 3 ($P < 0.001$; Figure 2b). T2 differed significantly between Outerbridge grades 0 and 2 ($P = 0.032$); 0 and 3 ($P < 0.001$); 1 and 3 ($P < 0.001$); and 2 and 3 ($P < 0.001$; Figure 2c).

Evaluation of the correlation of Outerbridge grade and MR parameters

Significant correlations were observed between the Outerbridge grades and the ADC ($R^2 = 0.9184$, $P < 0.001$; Figure 3a), and between the Outerbridge grades and T2 ($R^2 = 0.7883$, $P < 0.001$; Figure 3c). The FA ($R^2 = 0.6616$, $P < 0.05$; Figure 3b) was correlated slightly with the Outerbridge grades.

DT imaging of knee articular cartilage

A 21-year-old man sprained his knee while kickboxing. Five months later, he landed awkwardly in a hurdle touchdown and sprained his knee again. Giving way persisted and investigations revealed a right anterior cruciate ligament (ACL) injury and right medial meniscus injury. The patient was treated with ligament reconstruction and meniscal suture (Figure 4).

A 61-year-old man who had previously undergone meniscectomy in the right knee. He had pain on the inside of the right knee while walking and was being given oral analgesics treatment and injections by his local physician. However, the patient showed no improvement and was referred to our department for further examination. The patient was subsequently diagnosed with osteoarthritis of the right knee and underwent high tibial osteotomy (Figure 5).

Discussion

T2 mapping in the present study enabled discrimination between Outerbridge grades 0 and 2, 0 and 3, 1 and 3, and 2 and 3, thus allowing detection of moderate or severe cartilage damage. In DT imaging, the ADC enabled discrimination between grades 0 and 2, 0 and 3, 1 and 2, 1 and 3, and 2 and 3 cartilage damage relatively early,

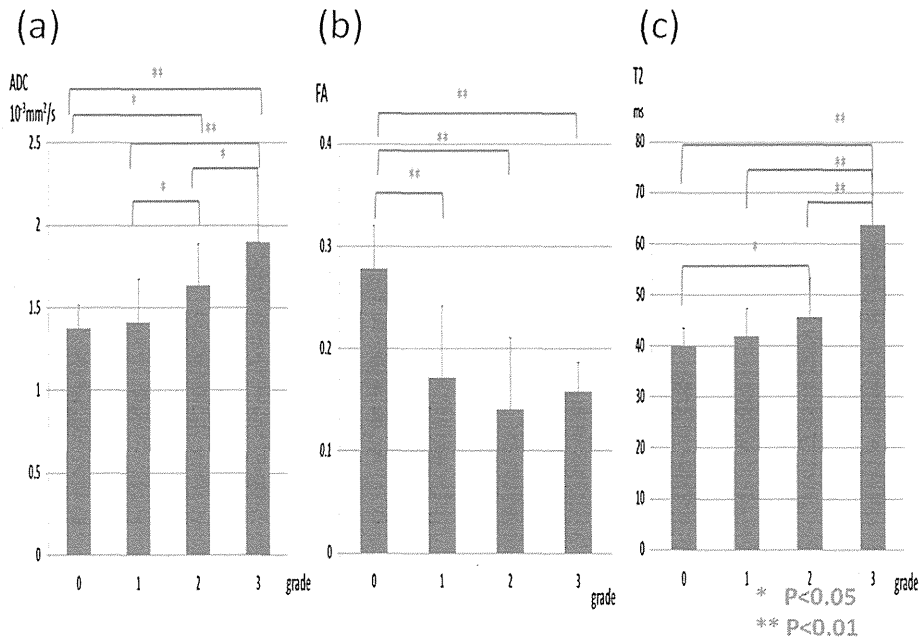

Figure 2 Comparisons of Outerbridge grade and the ADC, FA, and T2. (a) Significant differences in the ADC were observed between grades 0 and 2 ($P = 0.041$); 0 and 3 ($P < 0.001$); 1 and 2 ($P = 0.045$); 1 and 3 ($P < 0.001$); and 2 and 3 ($P = 0.028$). No significant difference was observed between grades 0 and 1. **(b)** Significant differences in the FA were observed between grades 0 and 1 ($P < 0.001$); 0 and 2 ($P < 0.001$); and 0 and 3 ($P < 0.001$). **(c)** Significant differences in T2 were observed between grades 0 and 2 ($P = 0.032$); 0 and 3 ($P < 0.001$); 1 and 3 ($P < 0.001$); and 2 and 3 ($P < 0.001$). No significant difference was noted between grades 0 and 1, 1 and 2.

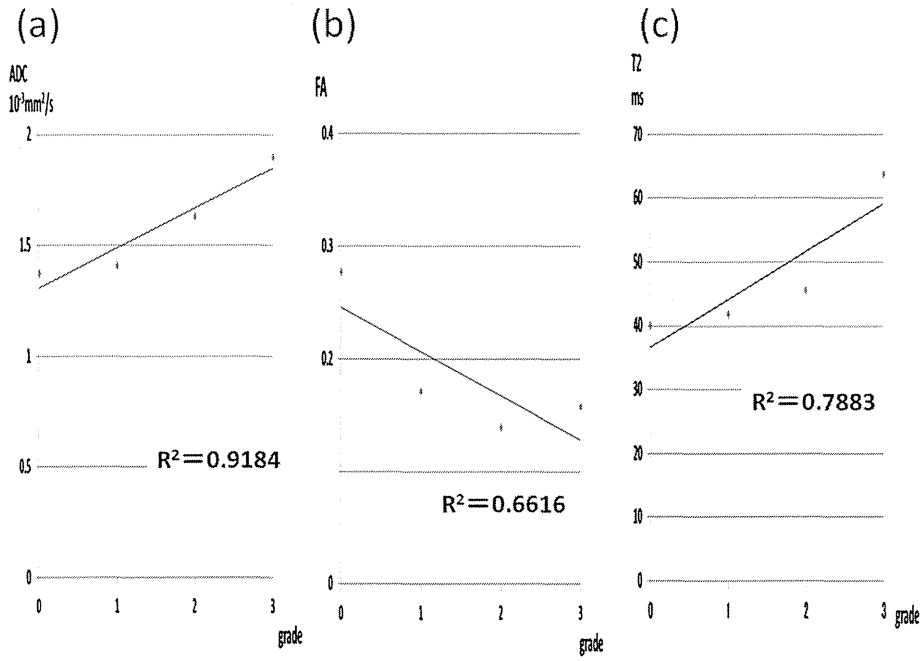

Figure 3 Relationship between Outerbridge grade and the ADC, FA, and T2. (a) A significant positive correlation was observed between the Outerbridge grade and the ADC ($R^2 = 0.9184$, $P < 0.001$). **(b)** The FA ($R^2 = 0.6616$, $P < 0.05$) was slightly correlated with the Outerbridge score. **(c)** A significant positive correlation was observed between Outerbridge grade and T2 ($R^2 = 0.7883$, $P < 0.001$).

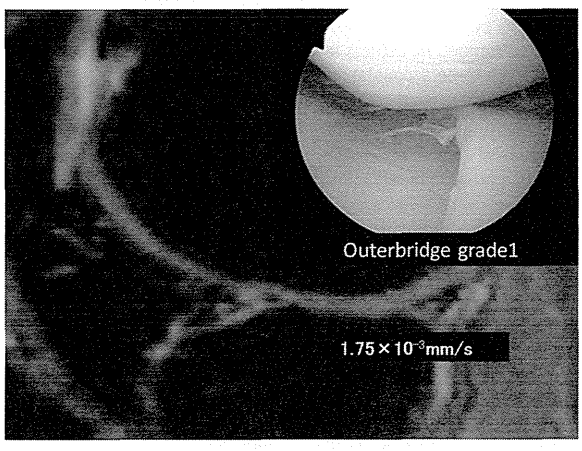

Figure 4 DT imaging in the early cartilage damage. The patient underwent surgery for right knee ACL and medial meniscus injury. In the inner femoral condyle, a cartilage crack caused by the medial meniscus rupture was observed to have Outerbridge grade 1 damage. The ADC for this area was measured as 1.75×10^{-3} mm^2/s.

and the FA allowed for discrimination between normal cartilage and damaged cartilage between grades 0 and 1, 0 and 2, and 0 and 3.

T2 mapping

Caution is needed during evaluation because T2 increases considerably with inclinations of about 55° in the direction of the static magnetic field (B0), and a magic angle effect is often observed in the posterior femoral condyle and at the top of the talus [3]. T2 has been reported to reflect the collagen fiber direction and articular cartilage water content. Previous studies that have investigated the use of T2 mapping to evaluate articular cartilage have found the technique to be useful, even for evaluating early stage cartilage damage [13-21]. However, Williams *et al.* [22] found no significant differences between ultrashort echo-time T2 mapping and standard T2 mapping of tissue samples with each grade of cartilage damage.

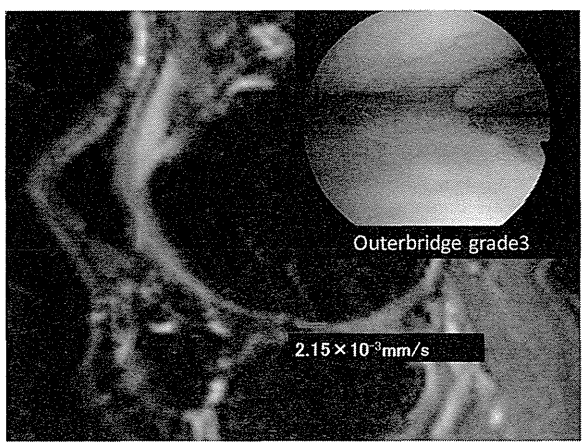

Figure 5 DT imaging in the severe cartilage damage. The patient underwent surgery for a right knee medial meniscus injury. Outerbridge grade 3 cartilage damage caused by the medial meniscus rupture was observed throughout the entire inner femoral condyle. The ADC for this area was measured as 2.15×10^{-3} mm^2/s.

The present study found significant differences between Outerbridge grades 0 and 2, 0 and 3, 1 and 3, 2 and 3, but no significant differences between grades 0 and 1, and 1 and 2. Threfore, although T2 mapping proved useful for evaluating moderate to severe cartilage damage, it was not useful for evaluating early stage cartilage damage. In T2 mapping, a breakdown of the collagen alignment within cartilage leads to an increase in T2, whereas a decrease in the content of proteoglycans, which form part of the extracellular matrix, has no effect [23,24]. T2 mapping can reflect collagen alignment accurately but may not detect early stage cartilage damage because proteoglycan depletion occurs before collagen depletion in patients with OA-induced cartilage damage [1].

DT imaging

DT imaging detects water molecule dispersion. In fibrous tissues, water molecule dispersion can occur only in the same direction as the fibers, indicating that the direction of water molecule movement matches fiber alignment. Accordingly, DT imaging can be used to evaluate the direction of articular cartilage collagen fibers and structural anisotropy. Normal articular cartilage exhibits isotropy [12], and cartilage matrix damage leads to anisotropy [22]. Similar to T2 mapping, the results of DT imaging can change according to cartilage depth. The ADC decreases with distance from the surface and toward the subchondral bone, whereas the FA increases closer to the subchondral bone [5]. In DT imaging, the ADC increases with depletion of cartilage proteoglycan and collagen [12,25], both of which are considered to reflect knee articular cartilage degeneration [15,26].

Raya *et al.* [5] collected human articular cartilage and compared the evaluations of the damaged regions between the ADC and actual samples. They found a sensitivity of 95% for cartilage damage detection and an accuracy of 63% for cartilage damage grading. The authors concluded that the ADC is useful for assessing cartilage damage. Meder *et al.* [27] treated cow knee articular cartilage with trypsin before conducting DT imaging and found that the ADC was higher after treatment than before treatment in the trypsin-treated cartilage. The ADC was also reported to increase in human articular cartilage after trypsin treatment [4]. Therefore, the ADC is considered to be useful for evaluating proteoglycan volume.

Few reports have shown that FA is useful for evaluating cartilage damage, and some have stated that the FA does not reflect proteoglycan volume because trypsin treatment barely affects it [4]. Raya *et al.* [26] compared

the FA of a normal and an OA knee joint using DTI, reporting that the FA in the OA group declined significantly compared with the normal group, with a sensitivity of 81% and a specificity of 83%. However, in contrast to our case, the evaluation for OA was carried out exclusively by X-*P* in this report, and it is unknown at which grade the evaluation was actually carried out. Moreover, Raya *et al.* [5,26] used 17.6 T and 7.0 T MRI, and they did not report the degree of evaluation that may be carried out with respect to cartilage evaluation upon MRI used in daily clinical practice.

Raya *et al.* [26] measured FA values in an OA group and a normal group, and reported significantly lower values in the OA group. However, no significant difference was observed in grades 1 to 3 of the OA group, and it was difficult to evaluate the cartilage damage solely from FA. According to the report by Deng *et al.* [28], the cartilage is regarded as having weak anisotropy compared with biological tissues, such as the brain and the heart. Consequently, it was believed that although a diagnosis of OA was possible via the investigation into the FA of this study, it was difficult to evaluate the extent of damage caused by OA.

In the ADC, we found significant differences between Outerbridge grades 0 and 2, 0 and 3, 1 and 2, 1 and 3, and 2 and 3. Although no significant difference was observed between grades 0 and 1, the ADC differed from T2 mapping in that it identified a significant difference between grades 1 and 2. Therefore, our results suggest that the ADC is useful for evaluating early stage cartilage damage. A strong correlation was observed between the Outerbridge grade and the ADC, suggesting that the ADC is useful for cartilage evaluation.

Conclusions

In our study, T2 mapping was useful for assessing moderate to severe cartilage damage (Outerbridge grade 2 and 3), and the ADC was useful for assessing relatively early stage cartilage damage (Outerbridge grades 1 and 2) and severe cartilage damage (Outerbridge grades 2 and 3). The FA can detect cartilage damage but cannot distinguish early cartilage damage from severe cartilage damage.

Abbreviations

ACL: Anterior cruciate ligament; ADC: Apparent diffusion coefficient; DT: Diffusion tensor; EPI: Echo planar imaging; FA: Fractional anisotropy; FOV: Field of view; MRI: Magnetic resonance imaging; NEX: Number of excitations; OA: Osteoarthritis; ROI: Region of interest; TE: Echo time; TR: Repetition time; TSE: Turbo spin echo; WFS: Water fat shift.

Competing interests

The authors declare that they have no competing interests.

Authors' contributions

MS, YI, TY, and JM contributed to the conception and design of the study. TU, KS, and TT acquired and analyzed the data. GM, TT, and KS performed the arthroscopic surgery and graded the cartilage damage. TU, TT, KS, and TY measured the areas of cartilage damage on the MRI. TU, MS, KS, and TT contributed to the interpretation of the data. TU wrote the first version of the manuscript, and all other authors revised it critically for important intellectual content. All authors read and approved the final manuscript. All authors agree to be accountable for all aspects of the work.

Acknowledgements

The authors wish to acknowledge Tomohiko Horie for technical assistance and for performing the MRI scans. Written informed consent was obtained from the patients for publication of their individual details and accompanying images in this manuscript. The consent form is held by the authors and is available for review by the Editor-in-Chief.

Author details

[1]Department of Orthopaedic Surgery, Surgical Science, Tokai University School of Medicine, 143 Shimokasuya, Isehara, Kanagawa 259-1193, Japan. [2]Department of Radiology, Specialized Clinical Science, Tokai University School of Medicine, 143 Shimokasuya, Isehara, Kanagawa 259-1193, Japan.

Received: 30 June 2014 Accepted: 12 February 2015
Published online: 21 February 2015

References

1. Blumenkrantz G, Majumdar S. Quantitative magnetic resonance imaging of articular cartilage in osteoarthritis. Eur Cell Mater. 2007;13:76–86.
2. Eckstein F, Burstein D, Link TM. Quantitative MRI of cartilage and bone: degenerative changes in osteoarthritis. NMR Biomed. 2006;19:822–54.
3. Breuseghem V. Ultrastructural MR imaging techniques of the knee articular cartilage: problems for routine clinical application. Eur Radiol. 2004;14:184–92.
4. Raya JG, Melkus G, Adam-Neumair S, Dietrich O, Mutzel E, Kahr B, et al. Change of diffusion tensor imaging parameters in articular cartilage with progressive proteoglycan extraction. Invest Radiol. 2011;46:401–9.
5. Raya JG, Melkus G, Adam-Neumair S, Dietrich O, Mutzel E, Reiser MF, et al. Diffusion-tensor imaging of human articular cartilage specimens with early signs of cartilage damage. Radiology. 2013;266:831–41.
6. Joseph KB, Harel N, Kim CY, Wang XX, Hasan O, Kauffman A, et al. Diffusion tensor imaging as a predictor of experimental spinal cord injury severity and recovery. Neurosurgery. 2013;60:175–6.
7. Cauley KA, Thangasamy S, Dundamadappa SK. Improved image quality and detection of small cerebral infarctions with diffusion-tensor trace imaging. Am J Roentgenol. 2013;200:1327–33.
8. Raya JG, Arnold AP, Weber DL, Filidoro L, Dietrich O, Neumair SA, et al. Ultra-high field diffusion tensor imaging of articular cartilage correlated with histology and scanning electron microscopy. Magn Reson Mater Phy. 2011;24:247–58.
9. de Visser SK, Bowden JC, Wentrup-Byrne E, Rintoul L, Bostrom T, Pope JM, et al. Anisotropy of collagen fibre alignment in bovine cartilage: comparison of polarized light microscopy and spatially resolved diffusion-tensor measurements. Osteoarthritis Cartilage. 2008;16:689–97.
10. Outerbridge RE, Westminster M, Columbia B. The etiology of chondromalacia patellae. J Bone Joint Surg. 1961;43:752–7.
11. Buckwalter JA, Mankin HJ. Articular cartilage II: Degeneration and osteoarthritis, repair, regeneration and transplantation. J Bone Joint Surg Am. 1997;79:612–32.
12. Burstein D, Gray ML, Hartman AL, Gipe R, Foy BD. Diffusion of small solutes in cartilage as measured by nuclear magnetic resonance (NMR) spectroscopy and imaging. J Orthop Res. 1993;11:465–78.
13. Dardzinski BJ, Laor T, Schmithorst VJ, Klosterman L, Graham TB. Mapping T2 relaxation time in the pediatric knee: feasibility with a clinical 1.5-T MR imaging system. Radiology. 2002;225:233–9.
14. Fragonas E, Mlynarik V, Jellus V, Micali F, Piras A, Toffanin R, et al. Correlation between biochemical composition and magnetic resonance appearance of articular cartilage. Osteoarthritis Cartilage. 1998;6:24–32.
15. Frank LR, Wong EC, Luh WM, Ahn JM, Resnick D. Articular cartilage in the knee: mapping of the physiologic parameters at MR imaging with a local gradient coil—preliminary results. Radiology. 1999;210:241–6.
16. Kwee TC, Takahara T, Ochiai R, Katahira K, Cauteren MV, Imai Y, et al. Whole-body diffusion-weighted magnetic resonance imaging. Eur J Radiol. 2009;70:409–17.
17. Mosher TJ, Dardzinski BJ, Smith MB. Human articular cartilage: influence of aging and early symptomatic degeneration on the spatial variation of T2–preliminary findings at 3 T. Radiology. 2000;214:259–66.

18. Nieminen MT, Rieppo J, Toyras J, Hakumaki JM, Silvennoinen J, Hyttinen MM, et al. T2 relaxation reveals spatial collagen architecture in articular cartilage: a comparative quantitative MRI and polarized light microscopic study. Magn Reson Med. 2001;46:487–93.
19. Nieminen MT, Toyras J, Rieppo J, Hakumaki JM, Silvennoinen J, Helminen HJ, et al. Quantitative MR microscopy of enzymatically degraded articular cartilage. Magn Reson Med. 2000;43:676–81.
20. Smith HE, Mosher TJ, Dardzinski BJ, Collins BG, Collins CM, Yang QX, et al. Spatial variation in cartilage T2 of the knee. J Magn Reson Imaging. 2001;14:50–5.
21. Xia Y, Moody JB, Alhadlaq H. Orientational dependence of T2 relaxation in articular cartilage: a microscopic MRI (microMRI) study. Magn Reson Med. 2002;48:460–9.
22. Williams A, Qian Y, Bear D, Chu CR. Assessing degeneration of human articular cartilage with ultra-short echo time (UTE) T2 mapping. Osteoarthritis Cartilage. 2010;18:539–46.
23. Borthakur A, Shapiro EM, Beers J, Kudchodkar S, Keeland JB, Reddy R. Sensitivity of MRI to proteoglycan depletion in cartilage: comparison of sodium and proton MRI. Osteoarthritis Cartilage. 2000;8:288–93.
24. Timothy JM, Bernard JD. Cartilage MRI T2 relaxation time mapping: overview and applications. Semin Musculoskelet Radiol. 2004;8:355–68.
25. Xia Y, Farquhar T, Burton-Wurster N, Vernier-Singer M, Lust G, Helinski L. Self-diffusion monitors degraded cartilage. Arch Biochem Biophys. 1995;323:323–8.
26. Raya JG, Horng A, Dietrich O, Krasnokutsky S, Beltran LS, Storey P, et al. Articular cartilage: in vivo diffusion-tensor imaging. Radiology. 2012;262:550–09.
27. Meder R, Visser SK, Bowden JC, Bostrom T, Pope JM. Diffusion tensor imaging of articular cartilage as a measure of tissue microstructure. Osteoarthritis Cartilage. 2006;14:875–81.
28. Deng X, Farley M, Nieminen MT, Gray M, Burstein D. Diffusion tensor imaging of native and degenerated human articular cartilage. Magn Reson Imaging. 2007;25:168–71.

Nagai et al. Arthritis Research & Therapy 2014, 16:427
http://arthritis-research.com/content/16/5/427

arthritis research&therapy

RESEARCH ARTICLE Open Access

Bevacizumab, an anti-vascular endothelial growth factor antibody, inhibits osteoarthritis

Toshihiro Nagai, Masato Sato*, Miyuki Kobayashi, Munetaka Yokoyama, Yoshiki Tani and Joji Mochida

Abstract

Introduction: Angiogenesis is an important factor in the development of osteoarthritis (OA). We investigated the efficacy of bevacizumab, an antibody against vascular endothelial growth factor and an inhibitor of angiogenesis, in the treatment of OA using a rabbit model of anterior cruciate ligament transection.

Methods: First, we evaluated the response of gene expression and histology of the normal joint to bevacizumab treatment. Next, in a rabbit model of OA induced by anterior cruciate ligament transection, we used macroscopic and histological evaluations and real-time polymerase chain reaction (PCR) to examine the responses to intravenous (systemic) administration of bevacizumab (OAB IV group). We also investigated the efficacy of intra-articular (local) administration of bevacizumab in OA-induced rabbits (OAB IA group).

Results: Histologically, bevacizumab had no negative effect in normal joints. Bevacizumab did not increase the expression of genes for catabolic factors in the synovium, subchondral bone, or articular cartilage, but it increased the expression of collagen type 2 in the articular cartilage. Macroscopically and histologically, the OAB IV group exhibited a reduction in articular cartilage degeneration and less osteophyte formation and synovitis compared with the control group (no bevacizumab; OA group). Real-time PCR showed significantly lower expression of catabolic factors in the synovium in the OAB IV group compared with the OA group. In articular cartilage, expression levels of aggrecan, collagen type 2, and chondromodulin-1 were higher in the OAB IV group than in the OA group. Histological evaluation and assessment of pain behaviour showed a superior effect in the OAB IA group compared with the OAB IV group 12 weeks after administration of bevacizumab, even though the total dosage given to the OAB IA group was half that received by the OAB IV group.

Conclusions: Considering the dosage and potential adverse effects of bevacizumab, the local administration of bevacizumab is a more advantageous approach than systemic administration. Our results suggest that intra-articular bevacizumab may offer a new therapeutic approach for patients with post-traumatic OA.

Introduction

Osteoarthritis (OA), the most common joint disease, is often given less attention than other diseases, such as cancer, because it is not a disorder directly associated with the sustainability of life. However, OA leads to severe joint dysfunction and pain, and a decline in the patient's quality of life with an associated decrease in the ability to perform activities of daily life. Patients with early to mid-stage OA are given pharmacological treatment for pain relief, although the long-term benefits have not been shown convincingly. Patients with advanced OA are indicated for total joint arthroplasty.

Articular cartilage is an avascular tissue comprising a sparse cell population with low mitotic activity, and its capacity for self-repair is limited. Therefore, mature articular cartilage shows limited capacity for regeneration after degeneration or injury. For this reason, various treatments have been developed with the aim of restoring tissue quality via regenerative methods. Techniques such as microfracture [1], mosaicplasty [2], cell transplantation [3,4], and the implantation of tissue-engineered cartilage with [5-7] or without [8-10] various scaffolding materials have received increasing attention. However, the restorable areas are limited and tend to be replaced with bone or fibrocartilage tissue.

Previously, we investigated the use of an osteochondral defect model to explore methods to repair cartilage defect

* Correspondence: sato-m@is.icc.u-tokai.ac.jp
Department of Orthopaedic Surgery, Surgical Science, Tokai University School of Medicine, 143 Shimokasuya, Isehara, Kanagawa 259-1193, Japan

sites. This was first accomplished by developing a three-dimensional, scaffold-free, tissue-engineered cartilage [9] that was transplanted into osteochondral defects to initiate cartilage differentiation [10]. This method achieved good restorative effects in the long term, allowing us to confirm that articular cartilage repair can be achieved during the early stage of transplantation [10]. We noted that reparative cells from marrow had acquired anti-angiogenic properties, and we hypothesized that better cartilage repair might be achieved by inhibiting the bioactivity of vascular endothelial growth factor (VEGF) in osteochondral defects. We later reported that intravenous administration of an antibody against VEGF contributed to articular cartilage repair in an osteochondral defect model [11].

In OA, new blood vessels from the subchondral bone breach the tidemark into cartilage [12], and it is thought that these blood vessels contribute to articular cartilage ossification [13] and lead to osteophyte formation around the cartilage [14]. Angiogenesis and inflammation are closely integrated processes in the pathogenesis of OA, which is associated with increased angiogenesis in the synovium [15]. Synovitis is also characteristic of rheumatoid arthritis (RA). Studies of angiogenesis that have compared the pathogenesis of RA and OA have concluded that angiogenesis correlates with the extent of synovial hyperplasia observed in these two diseases and that hyperplasia is most severe in RA but is also present in OA-affected joints [16,17]. Angiogenesis also results in innervation of the articular cartilage [18], which may provide a source of pain in OA patients. Thus, an angiogenesis inhibitor that could suppress synovitis, osteophyte formation, and pain is an attractive candidate for the treatment of OA.

Although an anti-VEGF antibody is an attractive target for the treatment of neovascular disease, several complications associated with its intravenous administration have been reported, including haemorrhage, thromboembolism, proteinuria, delayed wound healing, and hypertension [19]. In a recent study, we showed that the systemic intravenous administration of bevacizumab improved articular cartilage repair in an osteochondral defect model [11]. In the current study, we first determined how normal joint tissue responds to bevacizumab treatment. We then evaluated the effects of intravenous injection of bevacizumab in a rabbit model of OA by comparing the restorative changes in the cartilage of the synovium, subchondral bone, and articular joint in bevacizumab-treated and untreated rabbits. Following this, we compared the effects on healing induced by intra-articular administration with those induced by intravenous administration of bevacizumab (Figure 1).

Methods

Animals and surgical procedures

Animal experiments were approved by the ethics review board of Tokai University and were performed in accordance with the guidelines on animal use of Tokai University (Authorization Number 122083). Adolescent Japanese white rabbits, aged 16 to 18 weeks and weighing about 2.5 kg, were used in this study. These rabbits were purchased from a professional breeder (Tokyo Jiken Dobutsu, Tokyo, Japan). The rabbits were anaesthetized by exposure to sevoflurane and O_2 gas. Under sterile conditions, a medial parapatellar approach was used to release the joint capsule and to perform an anterior cruciate ligament transection (ACLT) [20]. After recovery from surgery, all animals were allowed to walk freely in their cages without any splints. Animals were sacrificed after the experiments by an overdose of intravenous anaesthesia.

Bevacizumab dose

Intravenous (systemic) administration of bevacizumab

The half-life of bevacizumab in the normal blood circulation is reportedly 21.3 days [21]. In humans, the approved dose of bevacizumab is 5 mg/kg, with a clinical administration interval of more than 2 weeks [19]. Bevacizumab is cross-reactive with rabbit VEGF, but its affinity for rabbit VEGF is one-eighth that for human VEGF [22]. Therefore, we investigated bevacizumab at a dose of 40 mg/kg administered on day 1 and again 2 weeks later.

Intra-articular (local) administration of bevacizumab

The local administration of bevacizumab is currently performed in ophthalmology clinics, in which the drug is injected into the vitreous body at a concentration of 25 mg/ml [23]. Intravitreal bevacizumab has been shown to be non-toxic to the retina and optic nerve at the 2.5 mg dose tested in animals [24]. We thus chose to administer 25 mg/ml into the articular capsule of OA rabbits. A volume of 1 ml was deemed suitable because this is typical for intra-articular injections in rabbits [25].

Experimental design

Experiment 1: normal versus normal bevacizumab

Twelve rabbits were used to investigate the effects of bevacizumab treatment on normal articular cartilage, synovium, and subchondral bone. Six rabbits were given 100 mg of bevacizumab intravenously on day 1 and then again 2 weeks later (normal bevacizumab group, n = 12 knees), and the other six rabbits were used as normal controls (normal group, n = 12 knees). All rabbits were sacrificed after 3 weeks to examine gene expression (normal bevacizumab group, n = 6 knees; normal group, n = 6 knees) and histology (normal bevacizumab group, n = 6 knees; normal group, n = 6 knees).

Experiment 2: OA versus OA intravenous bevacizumab

Twenty rabbits underwent bilateral ACLT. Ten rabbits were given an intravenous injection of 100 mg bevacizumab 1 week and 3 weeks after ACLT (OAB IV group).

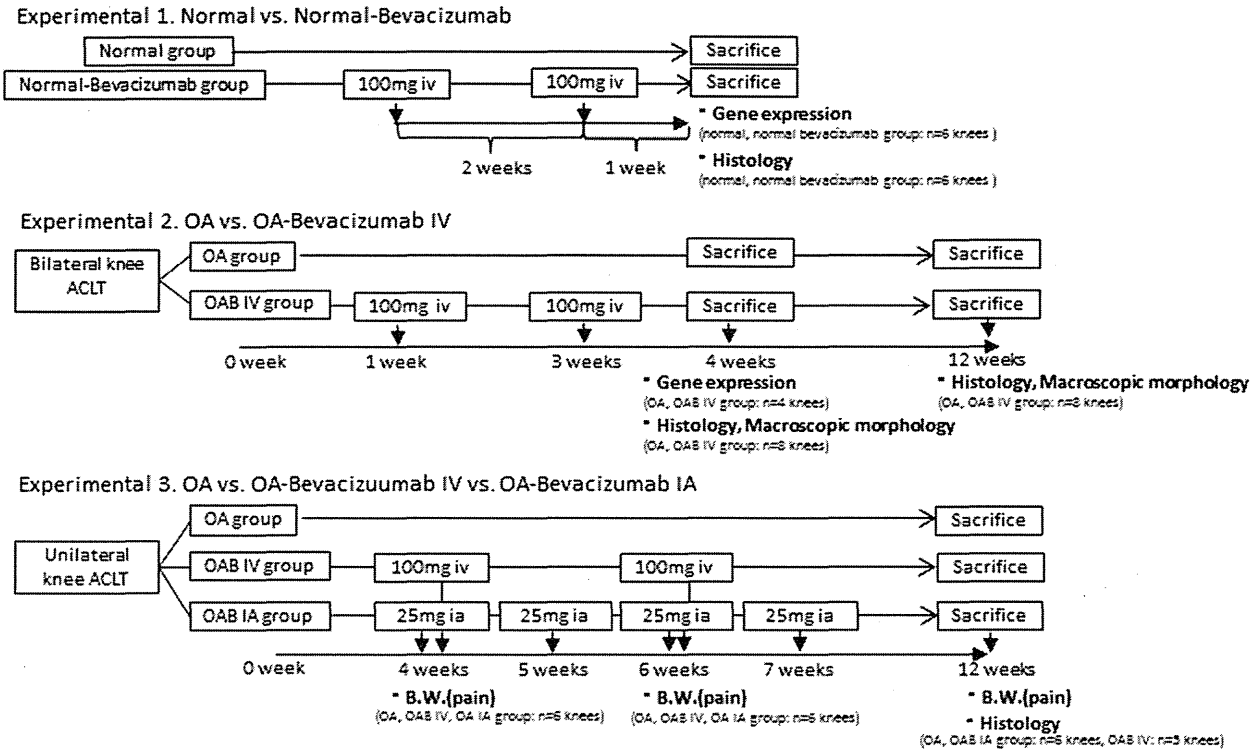

Figure 1 Study outline. This study comprised three experiments to assess the effects of bevacizumab in normal and rabbits with osteoarthritis (OA). Experiment 1: effects of bevacizumab treatment on normal articular cartilage, synovium, and subchondral bone were examined in 12 rabbits. Six normal (untreated) rabbits were given bevacizumab intravenously (iv) on day 1 and at 2 weeks (normal bevacizumab group, n = 12 knees), and the other six normal (untreated) rabbits were used as normal controls (normal group, n = 12 knees). All 12 rabbits were evaluated after 3 weeks to examine gene expression (normal bevacizumab group, n = 6 knees; normal group, n = 6 knees) and histology (normal bevacizumab group, n = 6 knees; normal group, n = 6 knees). Experiment 2: 20 rabbits were given bilateral anterior cruciate ligament transection (ACLT): 10 rabbits were given bevacizumab intravenously 1 week and 3 weeks after ACLT (OAB IV group), and 10 rabbits served as untreated OA controls (OA group). Rabbits were evaluated 4 weeks (n = 6 rabbits/group) and 12 weeks (n = 4 rabbits/group) after ACLT. Experiment 3: all rabbits were given unilateral knee ACLT. Intra-articular bevacizumab (25 mg) was injected 4 weeks after ACLT, then weekly until 7 weeks (OAB IA group). Intravenous bevacizumab (100 mg) was injected 4 and 6 weeks after ACLT (OAB IV group). Rabbits were evaluated 4, 6, and 12 weeks after ACLT. As the comparison, untreated unilateral ACLT rabbits were examined at the same times (OA group).

The other 10 rabbits were used as the untreated control group (OA group). It has been reported that, in unilateral and bilateral ACLT models, degenerative changes appear in the articular cartilage 4 weeks after surgery [26-28]. At 4 weeks, six rabbits from each group were sacrificed for histology (n = 8 knees) and gene expression (n = 4 knees). The remaining four rabbits in each group were sacrificed 12 weeks after ACLT, and their tissues were processed for histology (n = 8 knees).

Experiment 3: OA versus OA intravenous bevacizumab versus OA intra-articular bevacizumab

The final experiment was designed to compare intravenous with intra-articular administration of bevacizumab. In this experiment, ACLT was performed on 18 rabbits on only one knee per rabbit to measure pain behaviour in terms of weight-bearing asymmetry. Because ACLT was performed unilaterally in experiment 3, the progress of OA was predicted to be slower than that in the experiment involving bilateral ACLT. Therefore, we changed the timing of the administration of bevacizumab to 4 weeks after ACLT instead of 1 week. Six rabbits were given 100 mg of bevacizumab by intravenous injection 4 and 6 weeks after ACLT (OAB IV group, n = 6 knees, total dosage 200 mg), and six rabbits were given 25 mg bevacizumab by intra-articular injection 4, 5, 6, and 7 weeks after ACLT (OAB IA group, n = 6 knees, total dosage 100 mg). Six rabbits received no drug treatment (OA group, n = 6 knees). All animals were sacrificed 12 weeks after ACLT, and the knee joints were evaluated.

Morphology of osteophyte formation

The femoral condyles were examined macroscopically. Morphological changes were evaluated by two independent observers. The criteria for macroscopic grading were as follows: grade 0 (absent), grade 1 (mild osteophyte formation), grade 2 (moderate osteophyte formation), and grade 3 (severe osteophyte formation), as

described previously [29]. We included both osteophytes and chondro-osteophytes in our evaluation of osteophyte formation because both are regarded as neoplastic tissue caused by endochondral ossification as a result of angiogenesis in the articular margin associated with OA. The formation of chondro-osteophytes by hypertrophic chondrocytes reflects the process of endochondral ossification in the growth of osteophytes. The condyles were prepared for histological evaluation and gene expression analysis after morphological grading.

Histological examination

The distal parts of the femur were excised and fixed in 4% paraformaldehyde for 7 days. Each specimen was decalcified in a solution of 10% ethylenediaminetetraacetic acid in distilled water (pH 7.4) for 2 to 3 weeks, embedded in paraffin wax, and cut along the sagittal plane. Each section was stained with Safranin O. We evaluated OA repair sites at the medial femoral condyle semiquantitatively using a grading and staging system (Osteoarthritis Research Society International (OARSI) modified Mankin score [30]). This system includes six histological grades and four histological stages. The total score (grade score multiplied by stage score) ranges from 1 point (normal articular cartilage) to 24 points (no repair). The sections were examined blindly by two observers, and the scores were averaged to minimize observer bias. The synovium was sampled from the infrapatellar fat pad region. The synovial membrane was fixed in 4% paraformaldehyde for 7 days and subsequently embedded in paraffin. Each section was stained with H&E or Masson trichrome stain.

Gene analysis by real-time polymerase chain reaction (PCR)

The synovium was obtained from the infrapatellar fat pad region, articular cartilage was sampled from the femoral condyle, and subchondral bone was obtained from the femoral condyle with completely removed cartilage. Each construct was homogenized using a Cryo-Press (Microtec Nition, Chiba, Japan) in liquid nitrogen. Total RNA was isolated using the SV Total RNA Isolation System (Promega Corp., Madison, WI, USA), following the manufacturer's instructions. RNA quantification and quality were determined using the 260/280 nm ratio. Each RNA sample was then reverse-transcribed to cDNA using TaqMan Reverse Transcription reagents (Applied Biosystems, Foster City, CA, USA) in a thermocycler set at 42°C for 60 minutes and at 95°C for 5 minutes. The primer sequences used in this study are listed in Additional file 1: Table S1. Real-time PCR was performed in an ABI SDS 7300 real-time PCR system (Applied Biosystems) using SYBR Green Master Mix (Applied Biosystems). cDNA (2 μl) was added to bring the final volume of the real-time PCR sample to 25 μl. We then ran 35 to 45 amplification cycles: 2 minutes at 50°C, 10 minutes at 95°C, 15 s at 95°C, 1 minute at 60°C, and then 15 s at 95°C, 30 s at 60°C, and 15 s at 95°C (dissociation step). Normal articular cartilage, synovium, or subchondral bone was used as the reference for comparisons of gene expression between samples in experiments 1 and 2. The relative expression of the target mRNA was standardized to glyceraldehyde phosphate dehydrogenase, and the expression level was calculated using the $2^{-\Delta\Delta CT}$ values.

Pain evaluation

An incapacitance test meter (Linton Instrumentation, Norfolk, England) was used to identify and compare trends in the weight distribution ratio of the undamaged versus damaged limbs. The measurements were obtained from rabbits after they were transferred into the rabbit holder. The weight distribution of both hind legs was measured 10 times, and the following formula was used to calculate the damaged limb weight distribution ratios (%) obtained by loading the left and right limbs:

$$\text{Damaged limb weight distribution ratio } (\%) = \{\text{Damaged limb load } (g) / (\text{Undamaged limb load } (g) + \text{Damaged limb load } (g))\} \times 100.$$

Statistical analysis

All data are expressed as the mean ± SD. The nonparametric Mann-Whitney *U*-test was used to compare gene expression, histology, and gross morphology between two groups (experiments 1 and 2). The Kruskal-Wallis test followed by post hoc comparisons (Mann-Whitney *U*-test) was used to compare the pain evaluation test results and histological data between three groups (experiment 3). Differences were considered significant when *P*-values were <0.05 for comparisons between two groups or <0.017 for comparisons between three groups.

Results

Experiment 1: Effect of bevacizumab in normal tissues

Acute joint damage that occurs at the time of an injury initiates a sequence of events that can lead to progressive articular surface damage. Therefore, we sought to compare the gene expression and histological changes in the synovium, subchondral bone, and articular cartilage of knees between normal untreated (normal group) and bevacizumab-treated normal rabbits (normal bevacizumab group) (Figure 2). We administered bevacizumab intravenously and examined changes in the gene expression levels of various catabolic factors, including matrix metalloproteinase-3 (MMP3), MMP13, ADAMTS5 (a disintegrin and metalloproteinase with thrombospondin motifs-5), and interleukin-1β (IL-1β). In the synovium,

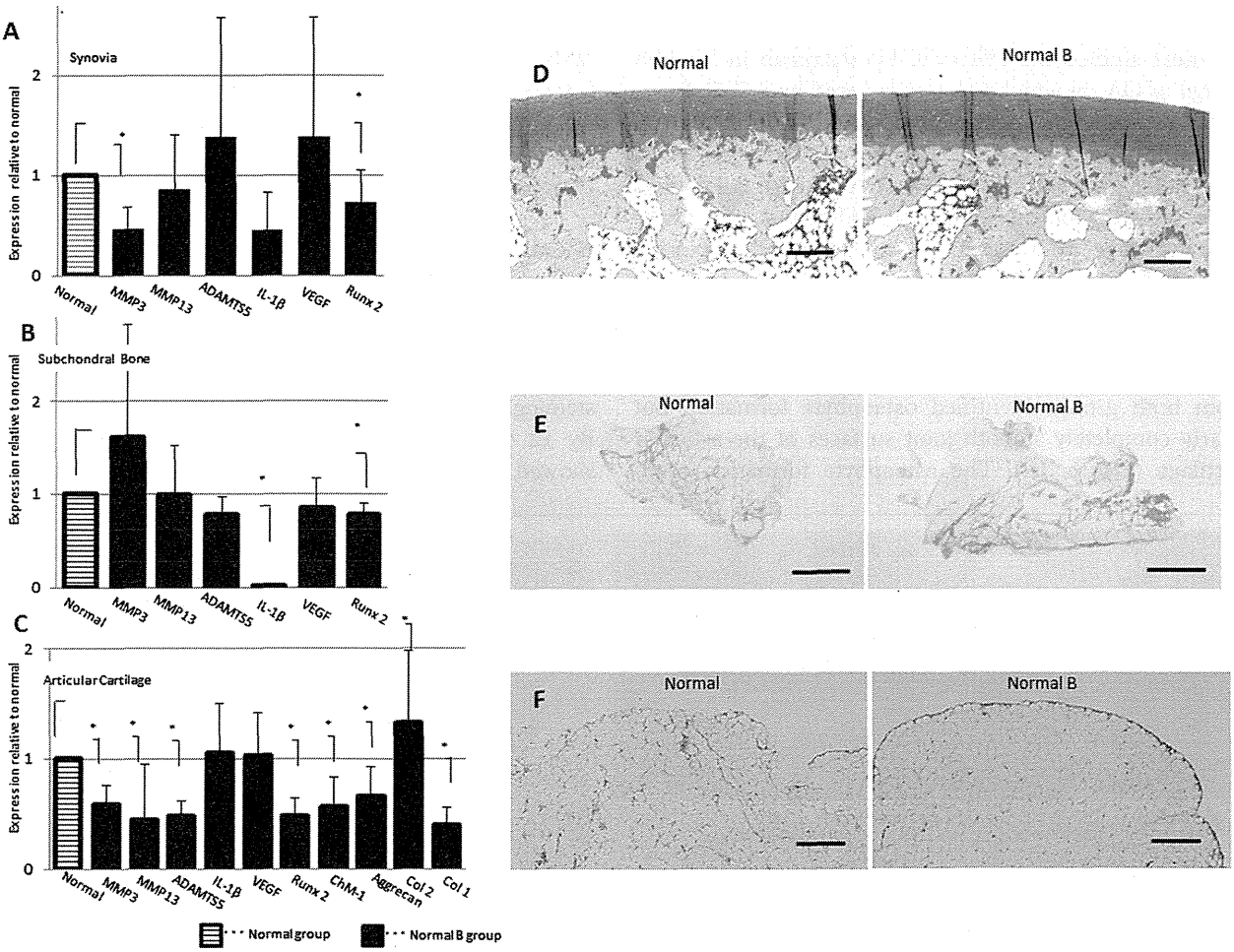

Figure 2 Comparison of gene expression and histology between the normal bevacizumab and normal groups (experiment 1). **(A)** Synovial gene expression. **(B)** Subchondral bone gene expression. **(C)** Articular cartilage gene expression. Gene expression data are expressed as mean ± SD (n = 6 knees). The y-axis is defined as follows: $2^{-\Delta CT}$ normal B target gene/$2^{-\Delta CT}$ normal target gene. *P <0.05 by the Mann-Whitney U-test. **(D)** Representative articular cartilage histology for the normal group (left side) and normal bevacizumab group (right side) stained with Safranin O. **(E)** Representative synovial histology for the normal group (left side) and normal bevacizumab group (right side) stained with H&E. **(F)** Higher magnifications of the image in **(E)** stained with H&E. Histology data were obtained from six knees per group. Bars = 1 mm **(E)**; bars = 300 μm **(D, F)**.

the expression of most genes tended to be lower in the normal bevacizumab group compared with the normal group; *MMP3* and *Runx2* expression levels were significantly lower in the normal bevacizumab group (Figure 2A). In subchondral bone, *IL1B* and *Runx2* expression levels were significantly lower in the normal bevacizumab group than in the normal group (Figure 2B). In articular cartilage, the expression levels of *MMP3*, *MMP13*, and *ADAMTS5* were significantly lower in the normal bevacizumab group compared with the normal group (Figure 2C). In the articular cartilage, the expression level of collagen type 2, the major collagen in cartilage, was elevated, but that of collagen type 1, the major collagen in bone and tendon, was lower in the normal bevacizumab group compared with the normal group. The expression levels of chondromodulin-1 (*ChM-1*), an endogenous anti-angiogenic factor, and aggrecan, the major structural protein in cartilage, were also lower in the normal bevacizumab group compared with the normal group. Intriguingly, *VEGF* mRNA expression was unaffected by intravenous administration of bevacizumab (Figure 2A-C).

Joints from the normal bevacizumab group showed smooth and uniform articular surfaces and Safranin O staining throughout the articular cartilage, similar to the appearance in the normal group (Figure 2D). In the synovium in the normal bevacizumab group, there was no synoviocyte hyperplasia or proliferation, or lymphoplasmacytic infiltration. One layer of synovial membrane with underlying adipose cells was apparent (Figure 2E, F).

Experiment 2: Comparison between OA and OA intravenous bevacizumab

We next studied the effects of bevacizumab in a rabbit model of OA, in which OA was induced by ACLT. Bevacizumab was administered 1 and 3 weeks after induction of OA into 10 rabbits (OAB IV group); 10 untreated OA-only rabbits served as controls (OA group). All rabbits were assessed for morphological differences and histological changes at 4 and 12 weeks, and gene expression changes were assessed at 4 weeks.

Morphology of osteophyte formation

Four weeks after ACLT, macroscopic evaluation of joints from both groups identified osteophyte formation but nearly completely smooth joint surfaces of the articular cartilage (Figure 3A). The osteophyte formation score did not differ between the OA group and the OAB IV group (Figure 3C). Twelve weeks after ACLT, the joint surfaces showed a marked progression of arthritis and osteophyte formation in the OA group. The joints from the OAB IV group retained smooth joint surfaces in most regions of the articular cartilage and had significantly less osteophyte formation (Figure 3B, C).

Histological evaluation of the articular cartilage

We evaluated the medial femoral condyle at the femoral-tibial (FT) site in the articular cartilage area. Four weeks after ACLT, histological assessment showed a loss of Safranin O-positive staining in the OA group, whereas staining was retained in the OAB IV group (Figure 3D). By 12 weeks after ACLT, the joints in the OA group showed delamination of the superficial layer, erosion of

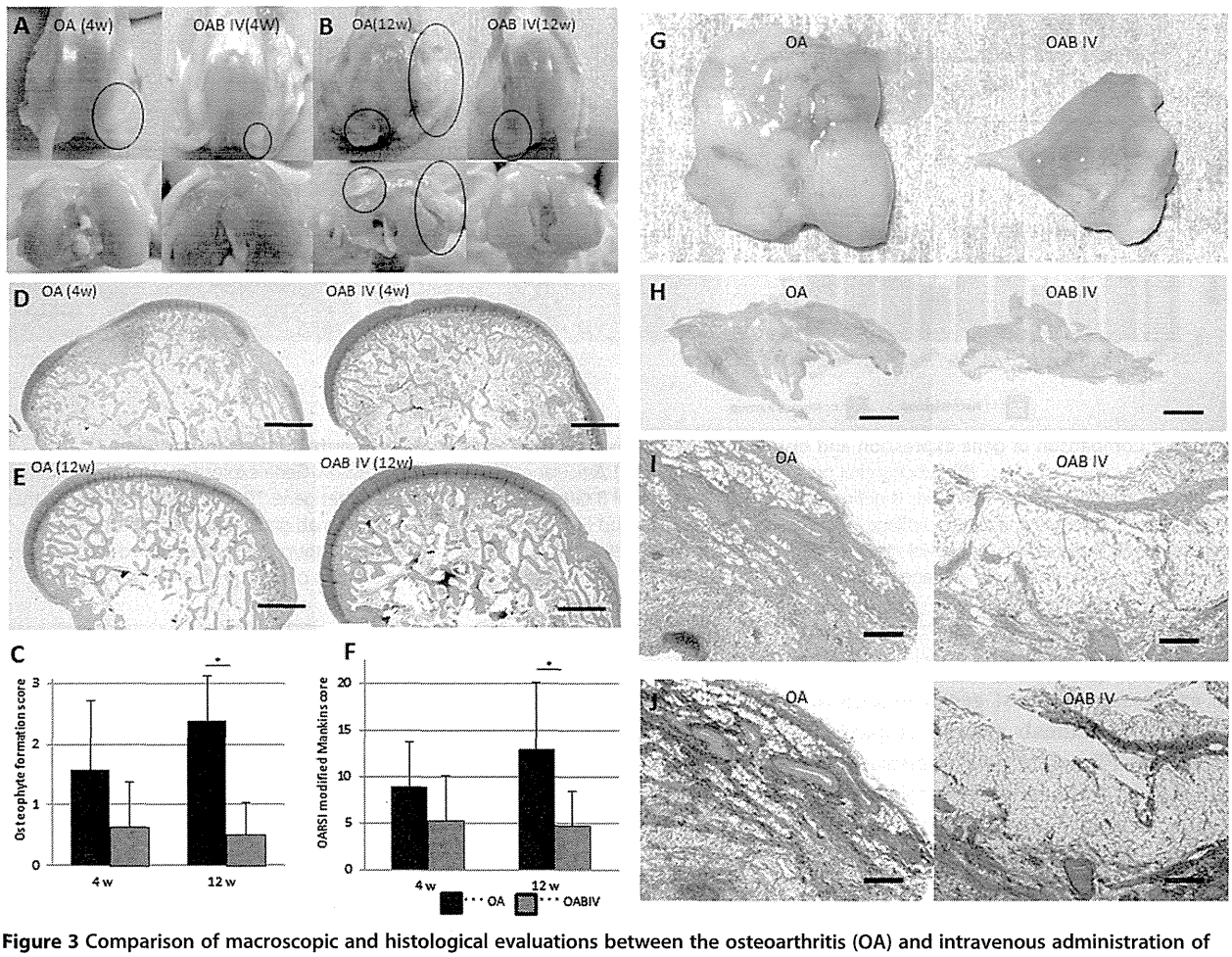

Figure 3 Comparison of macroscopic and histological evaluations between the osteoarthritis (OA) and intravenous administration of bevacizumab in OA (OAB IV) rabbits (experiment 2). (A) Macroscopic articular cartilage appearance 4 weeks after anterior cruciate ligament transection (ACLT). **(B)** Macroscopic appearance 12 weeks after ACLT. Circles indicate osteophyte formation. **(C)** Osteophyte formation scores 4 and 12 weeks after ACLT. Data are expressed as mean ± SD (n = 8 knees). Safranin O staining of hyaline cartilage 4 weeks **(D)** and 12 weeks **(E)** after ACLT. **(F)** Osteoarthritis Research Society International histological score 4 and 12 weeks after ACLT. **(G)** Macroscopic synovia appearance 4 weeks after ACLT. **(H)** Representative synovial histology for OA group (left side) and OAB IV group (right side) stained with H&E. Higher magnifications of the image shown in **(H)** stained with HE **(I)** and Masson trichrome **(J)**. Data are expressed as mean ± SD (n = 8 knees). *P <0.05 by the Mann-Whitney U-test. Bars = 1 mm **(D, E, H)**; bars = 300 μm **(I, J)**.

hyaline cartilage, and a lack of Safranin O staining. Joints from the OAB IV group showed smooth and uniform articular surfaces and Safranin O staining throughout the articular cartilage (Figure 3E). The total OARSI histological score did not differ between the OA and OAB IV groups at 4 weeks but was significantly lower in the OAB IV group than in the OA group at 12 weeks (Figure 3F).

Morphology and histology of the synovium

Four weeks after ACLT, the macroscopic appearance of the synovium showed enlargement with redness and recognized thick vascular invasion in the OA group. By contrast, in the OAB IV group, the synovium was preserved and appeared pale yellow, although a thin vascular invasion was apparent (Figure 3G). Synovial sections from the OA group showed severe synoviocyte hyperplasia with diffuse lymphoplasmacytic infiltration, blood vessel proliferation, and severe fibroblast proliferation with regression of adipose cells. These characteristics were present in the OAB IV group, but they were more moderate (Figure 3H, I, J). These results indicate that the structural damage was less severe in the OAB IV group than in the OA group.

Gene expression

We harvested the synovium, subchondral bone, and articular cartilage from the OA and the OAB IV groups 4 weeks after ACLT. We used real time PCR to assess changes in the expression of genes involved in anabolic and catabolic factors, and we compared these changes between the OA and OAB IV groups relative to the expression levels of the normal tissues at the baseline. *MMP13* gene expression in the normal synovium was about 10-fold higher in the OA group than in untreated animals. *MMP13* gene expression in the OAB IV group was one-tenth that in the OA group, a level that approximated the normal level. *ADAMTS5* gene expression did not increase in the OA group compared with the normal tissue but was significantly decreased by administration of bevacizumab (Figure 4A). The effect of bevacizumab on the OA synovial tissue differed from that

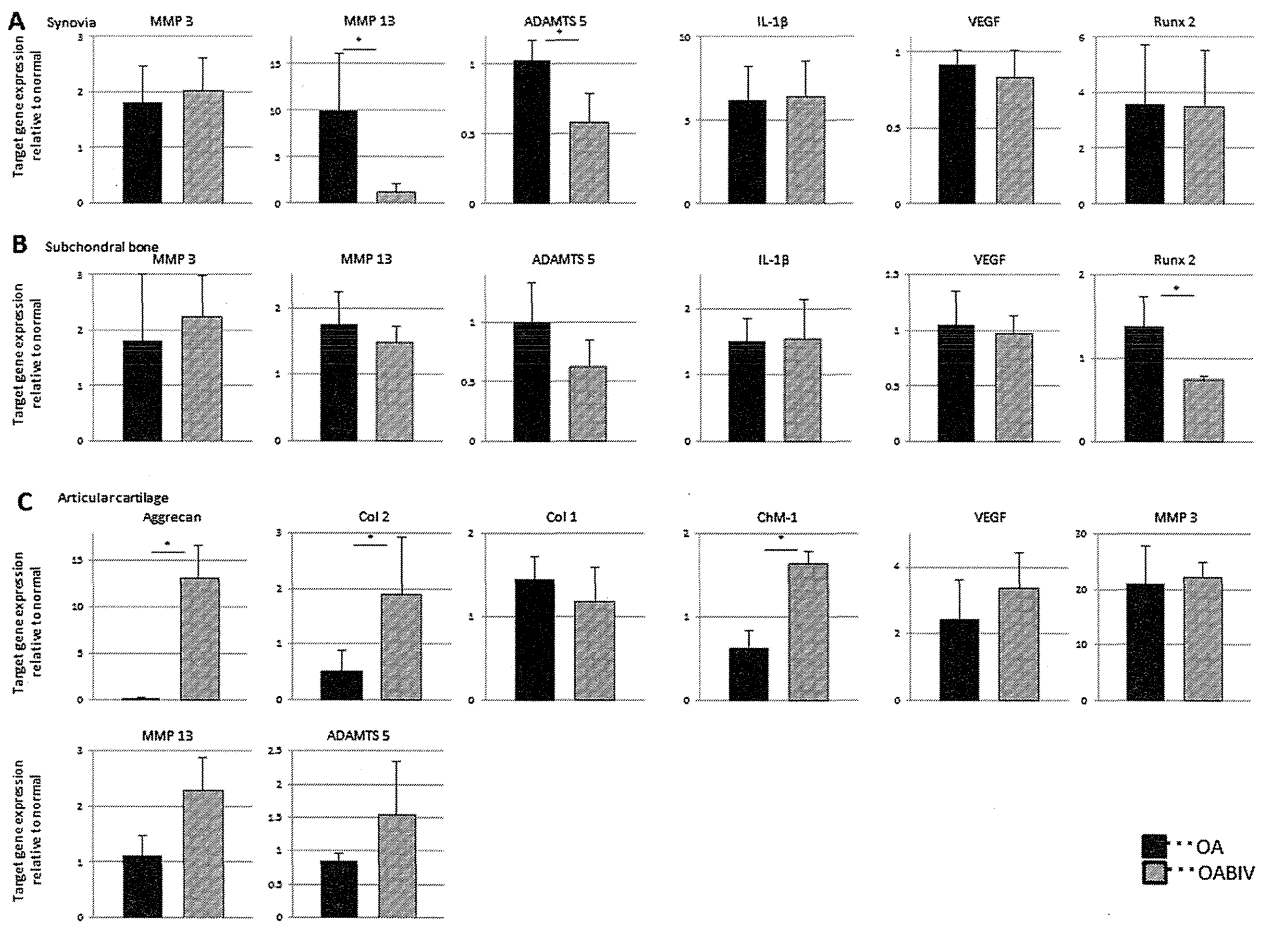

Figure 4 Comparison of relative gene expression levels between the osteoarthritis (OA) and intravenous administration of bevacizumab in OA (OAB IV) groups (experiment 2). (A) Synovial gene expression. **(B)** Subchondral bone gene expression. **(C)** Articular cartilage gene expression. The y-axis is defined as follows: $2^{-\Delta CT}$ OA or OAB IV target gene/$2^{-\Delta CT}$ normal target gene. The normal tissue is represented as 1 on the y-axis. Data are expressed as mean ± SD (n = 4 knees). *P <0.05 by the Mann-Whitney U-test.

in the normal synovium (Figure 2A). In subchondral bone, *Runx2* expression was also significantly lower in the OAB IV group compared with the OA group (Figure 4B). However, bevacizumab had a similar inhibitory effect on *Runx2* expression as in normal subchondral bone (Figure 2B).

Articular cartilage from the OAB IV group showed significantly 3.5-fold higher collagen type 2 gene expression compared with the OA group, and there was a tendency toward lower collagen type 1 gene expression in the OAB IV group compared with the OA group (Figure 4C). The patterns of changes in the expression of types 1 and 2 collagen genes were similar to those induced by bevacizumab treatment in normal articular cartilage (Figure 2C). Unlike the effect of bevacizumab in normal tissue, aggrecan and *ChM-1* gene expression levels were significantly higher in the OAB IV group compared with the OA group. By contrast, *MMP13* and *ADAMTS5* gene expression levels were about 2.0-fold higher and *VEGF* gene expression level 1.4-fold higher in the OAB IV group than in the OA group, but this increase was not significant. *MMP3* gene expression levels did not differ between the OAB IV group and the OA group.

Experiment 3: differences between intravenous and intra-articular administration of bevacizumab in a model of OA

Damaged limb weight distribution ratio (%)

A comparison of the weight distribution ratio between the three groups (OA, OAB IV, and OAB IA) following bevacizumab treatment is shown in Figure 5A. Up to 6 weeks, the rabbit weight distribution ratio did not differ between the three groups. However, by 12 weeks, rabbits in the OAB IA group showed a satisfactory improvement in the damaged limb weight distribution ratio, whereas rabbits in the OA and OAB IV groups failed to show such improvement. The OAB IA group showed significant improvement compared with the OA group (Figure 5A). Unfortunately, one rabbit from the OAB IV group developed diarrhoea and lost weight, and this rabbit died from complications involving digestion at 8 weeks.

Histological evaluation

Because unilateral ACLT was performed, the OA change was not as progressive at the FT site compared with that observed in rabbits that had received the bilateral ACLT in experiment 2. Therefore, we divided the distal portion of the femur into the FT site, femoral-patellar (FP) site, and corner site, which was between FP and FT (Figure 5B). In the OA group, diminished Safranin O staining and clear degeneration of the cartilage were observed at the FT site. Only minimal Safranin O staining was observed at the corner and FP sites (Figure 5C). By contrast, in the OAB IV group, matrix staining was strong at the FT site throughout the thickness of the cartilage and was stronger at the corner and FP sites compared with the OA group. Some matrix staining depletion was observed within the upper third of the cartilage at the corner site and within the full thickness of the cartilage within the FP site (Figure 5D). In the OAB IA group, matrix staining depletion was minimal at all three sites, and staining was observed throughout the full thickness of the tissue (Figure 5E). As expected, the OARSI histological score for Safranin O staining at the FT site did not differ significantly between the three groups (Figure 5F). However, at the corner and FP sites, the histological score was significantly lower in the OAB IA group than in the OA group (Figure 5G, H). These results indicate that the OAB IA group had less OA progression compared with the OAB IV and OA groups.

Discussion

We previously demonstrated that the intravenous administration of bevacizumab repaired articular cartilage in an osteochondral defect model [11]. Based on those results, the present study was designed as three separate experiments to (1) assess the effect of bevacizumab in normal joints; (2) clarify the therapeutic efficacy of the intravenous administration of bevacizumab in OA joints; and (3) evaluate the effects of a systemic versus local administration of bevacizumab in OA joints.

The intravenous administration of 100 mg of bevacizumab for a period of 2 weeks did not lead to inflammation or angiogenic effects in the three tissue types in the normal joint as determined by histological and gene expression in experiment 1. The expression of the genes for some anabolic and catabolic factors was suppressed by administration of bevacizumab in normal articular cartilage. This environment may be the extremely stable hypometabolism, rather than the toxicity to cartilage with bevacizumab.

Anderson *et al.* recently reported that early molecular interventions can limit cartilage degradation by minimizing the extent of tissue damage and can help accelerate healing by decreasing the inflammatory response [31]. In the current study, early intervention by intravenous administration of bevacizumab appeared to contribute to a reduction in articular cartilage degeneration, osteophyte formation, and synovitis, as determined macroscopically and histologically in experiment 2.

We performed PCR analyses to assess whether bevacizumab has preventive effects on the whole joint (that is, by comparing the results of experiments 1 and 2). In the synovium, *MMP13* and *ADAMTS5* expression levels were significantly lower in the OAB IV group than in the OA group. Although bevacizumab did not decrease *IL1B* expression significantly, we suggest that the decrease in *MMP13* and *ADAMTS5* expression levels contributed to the absence of synovitis.

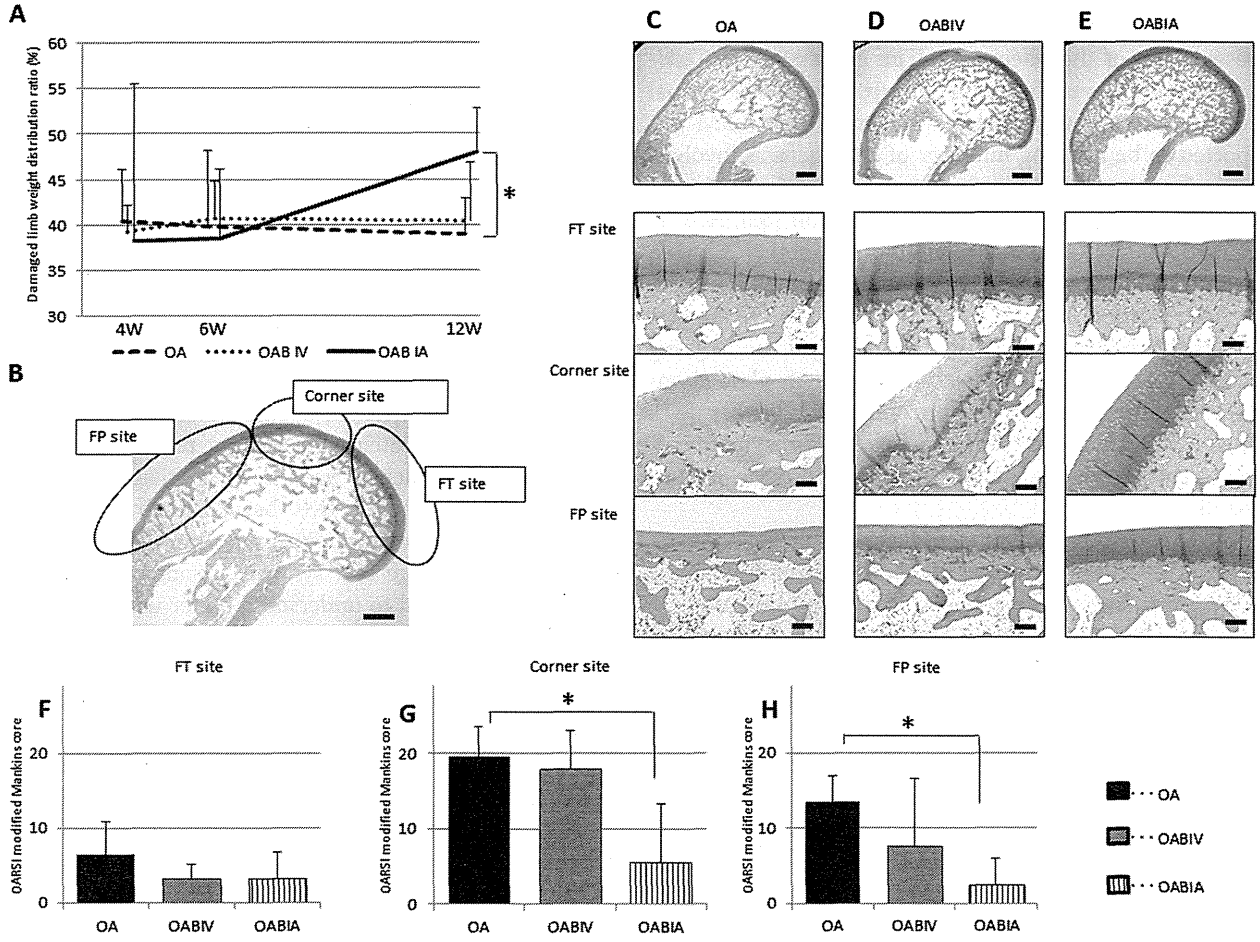

Figure 5 Comparison of pain and histological evaluations between osteoarthritis (OA), intravenous administration of bevacizumab in OA (OAB IV), and intra-articular administration of bevacizumab in OA (OAB IA) groups (experiment 3). (A) An incapacitance test meter was used to investigate the pain-ameliorating effects of treatment. The damaged limb weight distribution ratio (%) = {Damaged limb load (g)/(Undamaged limb load (g) + Damaged limb load (g))} × 100. The damaged limb weight distribution ratios 4, 6, and 12 weeks after surgery are shown. Data are expressed as mean ± SD (4 and 6 weeks after surgery: for each group, n = 6 knees; 12 weeks after surgery: OA and OAB IA groups, n = 6 knees, OAB IV group, n = 5 knees). *P <0.05 (Kruskal-Wallis post hoc test and Mann-Whitney U-test). **(B)** Distribution of femoral-patellar (FP), corner, and femoral-tibial (FT) sites. Safranin O-stained sections of articular cartilage. Bar = 1 mm. Representative Safranin-O-stained sections for the **(C)** OA, **(D)** OAB IV, and **(E)** OAB IA groups. Top row, overview of the distal femur. Bar = 1 mm. Second, third, and fourth rows, enlarged images of the FT site, corner site, and FP site. Bar = 250 μm. Osteoarthritis Research Society International histological scoring was performed at the **(F)** FT, **(G)** corner, and **(H)** FP sites. Data are mean ± SD (OA and OAB IA groups: n = 6 knees; OAB IV group: n = 5 knees). *P <0.05 (Kruskal-Wallis post hoc test and Mann-Whitney U-test).

Higher VEGF mRNA and protein levels have been reported in the synovial tissue of patients with inflammatory joint disease who required synovectomy compared with healthy control subjects [32]. Acute joint damage that occurs at the time of an injury initiates a sequence of events that can lead to progressive articular surface damage [31]. Subsequently, fragments of cartilage can induce synovitis in these patients [33]. In this study, damage to the articular surface led to an elevation in *VEGF* expression in the articular cartilage. In the synovium, there was a strong increase in the expression of *MMP* and *IL1B*, which indicates inflammation, but *VEGF* expression, which represents angiogenesis, was unchanged. This is probably because our study examined the early stages of OA (4 weeks after ACLT). Therefore, it seems likely that *VEGF* expression in the synovial tissue was not influenced by bevacizumab treatment.

Runx2 is the master gene of bone formation and contributes to sclerosis in subchondral bone and the formation of osteophytes [34]. From the early stages in our model, we observed a significant decrease in *Runx2* expression with bevacizumab treatment, suggesting that bevacizumab contributes to the inhibition of osteosclerosis in the subchondral bone and inhibits osteophyte formation.

In this study, the expression of both *VEGF* and *ChM-1* was examined in the articular cartilage. We consider that

the balance between angiogenic and anti-angiogenic factors is important to articular chondrocyte survival and preservation of the phenotype. The expression of *ChM-1*, which was lower in the OA group than in the normal group, increased with bevacizumab treatment. ChM-1 is reported to be a strong inhibitor of angiogenesis involved in the development of bone and regulation of vascular invasion during endochondral bone formation [35]. Articular cartilage contains considerable amounts of ChM-1, which should induce the chondrocyte phenotype [36]. It has been posited that the development of the OA phenotype might result from articular chondrocytes undergoing a differentiation route reminiscent of growth plate chondrocytes and expressing hypertrophy-like changes [37]. Thus, ChM-1 may act to prevent chondrocyte hypertrophy and to stabilize the articular chondrocyte phenotype [38].

VEGF is necessary for chondrocyte survival during cartilage development [39]. In an osteochondral defect model, we showed previously that administration of bevacizumab caused ChM-1 to accumulate in the interterritorial space of the repaired matrix surrounding the chondrocytes, which expressed VEGF [11]. In the articular cartilage, although *VEGF* expression was 2.4-fold higher in the OA group than in normal tissue from untreated rabbits, bevacizumab did not significantly alter *VEGF* expression.

The gene expression levels of the anabolic factors aggrecan and collagen type 2 were significantly higher in the OAB IV group than in the OA group. Interestingly, the gene expression of the catabolic factors in the articular cartilage, MMP13 and ADAMTS5, were higher in the OAB IV group than in the OA group, although this difference was not significant. Because this study was performed *in vivo*, we consider that the expression of the catabolic genes may have led to degradation of the existing matrix and subsequent proliferation and synthesis of new matrix in the limited articular cartilage space. The increase in *ChM-1* expression in response to bevacizumab may have increased the anabolic and catabolic factors, leading to proliferation and synthesis of new matrix *in vivo*. Interestingly, however, in normal articular cartilage, *ChM-1* expression was decreased by administration of bevacizumab (Figure 2C). Kitahara *et al.* suggested that ChM-1 acts to inhibit vascular invasion in the immature state of articular cartilage and that ChM-1 levels decrease gradually with age thereafter [40]. Such findings suggest a regulatory role of ChM-1 in vascular invasion; that is, exposure of tissues to angiogenesis factors is reduced in mature articular cartilage concomitant with a reduction in ChM-1 at both the protein and gene expression levels. In other words, ChM-1 appears to decrease at the non-angiogenic sites. In the current study, it is possible that angiogenic factors were reduced at the protein level after bevacizumab administration in the normal articular cartilage; if so, *ChM-1* gene expression would have also decreased following the administration of bevacizumab in normal articular cartilage.

One limitation of this study is that we did not measure VEGF protein levels in the tissue before and after treatment with bevacizumab, which is important when examining the treatment effects of bevacizumab. In this experiment, intermittent treatment with bevacizumab induced less OA progression, as shown by both histological and gene expression assays, through increases in the gene expression of *ChM-1* and *VEGF* in the articular cartilage and decreases in the gene expression of *MMP 13* and *ADAMTS5* in the synovium. Thus, although bevacizumab bound to VEGF protein, this did not prevent the expression of *VEGF*, which is needed for cartilage survival. In addition, it is thought that bevacizumab functions to modify the local environment by preventing angiogenesis in articular cartilage and synovial inflammation. Further research is required to understand better what determines the magnitude of the increase in ChM-1 at both the protein and gene expression levels in response to bevacizumab in OA tissues. It is important to understand the pharmacokinetic profile of the drug if we are to optimize dosing regimens for patients and to obtain a better assessment of its safety profile.

The second limitation of this study is that we did not monitor the dose-response relationship for bevacizumab because a sufficient preventive effect against OA progression occurred with the intravenous administration of 200 mg (2 × 100 mg) of bevacizumab and intra-articular administration of 100 mg (4 × 25 mg) of bevacizumab. In the absence of intravenous administration of bevacizumab, intra-articular administration may lead to bevacizumab being absorbed by the highly vascular synovial membrane and then circulated throughout the whole body. Therefore, some of the effects of the intra-articular injection of bevacizumab may be attributable to its presence in the systemic circulation. Future studies should assess the effects of tapered dosages of bevacizumab and the optimal systemic dosage.

We have shown here that intravenous administration of bevacizumab is associated with reductions in synovitis, articular degeneration, and osteophyte formation in an ACLT model of OA. Systemic bevacizumab-treated joints also generally showed greater aggrecan preservation, as indicated by the intensity of Safranin O staining of the articular cartilage (Figure 3). These results are promising for translating this study into the clinical setting. As described earlier, there are numerous potential side effects of systemic administration of bevacizumab. It is likely that the intra-articular administration of bevacizumab will decrease the risk of these adverse events. In this study, there was no disadvantage associated with

intra-articular administration of bevacizumab compared with intravenous administration. The total dose of the drug given to the OAB IA group was half that given to the OAB IV group. Moreover, the animals exhibited significantly less pain in the OAB IA group. Bonnet and Walsh commented that angiogenesis may introduce sensory nerves into the aneural cartilage and that inflammation can sensitize nerves present in the joint [33]. It is believed that the intra-articular administration of bevacizumab inhibits angiogenesis and inflammation, thereby reducing OA progression and providing pain relief. Because ACLT was performed unilaterally in experiment 3, the progression of OA was slower than that in experiment 2, which involved bilateral ACLT. Similar to experiment 2, the differences in the histological score and pain behaviour between the OA and OAB IV groups in experiment 3 will seem to occur after 12 weeks. Intravenous administration of bevacizumab is a promising treatment option for polyarthritis, whereas intra-articular administration might be recommended for patients with single-site arthritis.

Conclusions

In conclusion, we show that bevacizumab reduced synovitis, osteophyte formation, and cartilage degradation in a rabbit model of OA. Importantly, intra-articular administration of bevacizumab also reduced pain behaviour. Because bevacizumab was administered before the development of structurally severe OA, its effects might reflect changes in synovitis rather than direct effects on cartilage pathogenesis. Our findings indicate that early intervention by the administration of bevacizumab following an ACL injury may be beneficial in retarding the development of post-traumatic OA.

Additional file

Additional file 1: List of primers used in real-time PCR.

Abbreviations

ACLT: anterior cruciate ligament transection; ADAMTS5: A disintegrin and metalloproteinase with thrombospondin type 1 motif-5; ChM-1: chondromodulin-1; ACL: anterior cruciate ligament; FP: femoral-patellar; FT: femoral-tibia; H&E: haematoxylin and eosin; IL-1β: interleukin-1β; MMP: matrix metalloproteinase; OA: osteoarthritis; OAB IA: intra-articular administration of bevacizumab in OA; OAB IV: intravenous administration of bevacizumab in OA; OARSI: Osteoarthritis Research Society International; PCR: polymerase chain reaction; RA: rheumatoid arthritis; Runx2: runt-related transcription factor-2; VEGF: vascular endothelial growth factor.

Competing interests

The authors confirm that no competing interests of any kind exist for any of the authors, not only financial conflicts of interest. The authors declare that they applied for a patent relating to the content of the manuscript in Japan but did not receive any reimbursements, fees, funding, or salary from an organization. The competitive companies developing or selling anti-VEGF drugs (for example, Novartis, Wyeth, Bayer Schering) may keep them in check.

Authors' contributions

TN carried out the animal experiment, performed the statistical analyses, has been involved in drafting the manuscript and revising it critically for important intellectual content. MS has made substantial contributions to conception and design, interpretation of data, helped to draft the manuscript, and also agreed to be accountable for all aspects of the work in ensuring that questions related to the accuracy or integrity of any part of the work had been appropriately investigated and resolved. MK participated in the animal experiment, performed the PCR analyses and has been involved in drafting the manuscript. MY performed histological examinations and participated in PCR analyses and has been involved in drafting the manuscript. YT performed histological examinations and participated in the statistical analyses and has been involved in drafting the manuscript. JM participated in the design and coordination of the study and agreed to be accountable for all aspects of the work in ensuring that questions related to the accuracy or integrity of any part of the work had been appropriately investigated and resolved. All authors read and have given final approval of the version to be published.

Acknowledgements

This research was supported partly by Grants-In-Aid for Scientific Research from the Ministry of Education, Culture, Sports, Science and Technology.

Received: 16 November 2013 Accepted: 13 August 2014
Published online: 18 September 2014

References

1. Steadman JR, Rodkey WG, Briggs KK, Rodrigo JJ: **The microfracture technic in the management of complete cartilage defects in the knee joint. [Article in German].** *Orthopade* 1999, **28**:26–32.
2. Szerb I, Hangody L, Duska Z, Kaposi NP: **Mosaicplasty: long-term follow-up.** *Bull Hosp Jt Dis* 2005, **63**:54–62.
3. Brittberg M, Lindahl A, Nilsson A, Ohlsson C, Isaksson O, Peterson L: **Treatment of deep cartilage defects in the knee with autologous chondrocyte transplantation.** *N Engl J Med* 1994, **331**:889–895.
4. Moseley JB Jr, Anderson AF, Browne JE, Mandelbaum BR, Micheli LJ, Fu F, Erggelet C: **Long-term durability of autologous chondrocyte implantation: a multicenter, observational study in US patients.** *Am J Sports Med* 2010, **38**:238–246.
5. Buckwalter JA, Lohmander S: **Operative treatment of osteoarthrosis. Current practice and future development.** *J Bone Joint Surg Am* 1994, **76**:1405–1418.
6. Freed LE, Grande DA, Lingbin Z, Emmanual J, Marquis JC, Langer R: **Joint resurfacing using allograft chondrocytes and synthetic biodegradable polymer scaffolds.** *J Biomed Mater Res* 1994, **28**:891–899.
7. Marcacci M, Berruto M, Brocchetta D, Delcogliano A, Ghinelli D, Gobbi A, Kon E, Pederzini L, Rosa D, Sacchetti GL, Stefani G, Zanasi S: **Articular cartilage engineering with Hyalograft C: 3-year clinical results.** *Clin Orthop Relat Res* 2005, **435**:96–105.
8. Mainil-Varlet P, Rieser F, Grogan S, Mueller W, Saager C, Jakob RP: **Articular cartilage repair using a tissue-engineered cartilage-like implant: an animal study.** *Osteoarthr Cartil* 2001, **9**:S6–S15.
9. Nagai T, Furukawa KS, Sato M, Ushida T, Mochida J: **Characteristics of a scaffold-free articular chondrocyte plate grown in rotational culture.** *Tissue Eng Part A* 2008, **14**:1183–1193.
10. Nagai T, Sato M, Furukawa KS, Kutsuna T, Ohta N, Ushida T, Mochida J: **Optimization of allograft implantation using scaffold-free chondrocyte plates.** *Tissue Eng Part A* 2008, **14**:1225–1235.
11. Nagai T, Sato M, Kutsuna T, Kokubo M, Ebihara G, Ohta N, Mochida J: **Intravenous administration of anti-vascular endothelial growth factor humanized monoclonal antibody bevacizumab improves articular cartilage repair.** *Arthritis Res Ther* 2010, **12**:R178.
12. Walsh DA, Haywood L: **Angiogenesis: a therapeutic target in arthritis.** *Curr Opin Investig Drugs* 2001, **2**:1054–1063.
13. Walsh DA, Bonnet CS, Turner EL, Wilson D, Situ M, McWilliams DF: **Angiogenesis in the synovium and at the osteochondral junction in osteoarthritis.** *Osteoarthr Cartil* 2007, **15**:743–751.
14. Pufe T, Petersen W, Tillmann B, Mentlein R: **The splice variants VEGF121 and VEGF189 of the angiogenic peptide vascular endothelial growth factor are expressed in osteoarthritic cartilage.** *Arthritis Rheum* 2001, **44**:1082–1088.